factor (20 ng/mL; Cell Signaling Tech, Danvers, MA, USA), basic fibroblast growth factor (10 ng/mL; PeproTech, London, UK) and B27 supplements (1:50; Gibco). Capan-1 cells were cultured for 7 days. Immunofluorescence staining was performed on spheres in culture to identify CD133 expression. Cells were fixed with 10% formalin prior to immunostaining, then incubated with anti-CD133 mAb for 2 h at 37°C and subsequently washed three times with PBS containing 2% FBS. Next, the cells were incubated for 1 h with PE-conjugated anti-mouse secondary antibodies. Nuclear was stained by DAPI. Finally, the stained cells were viewed under a confocal laser scanning microscope (Olympus, Tokyo, Japan). The negative control groups contained cells stained only with the secondary antibody.

Migration and invasion assays. In total, 5×10^4 cells were seeded in serum-free medium into 24-well Falcon migration inserts (8 μm pore size). Inserts were placed in Falcon companion plates containing 10% FBS and incubated for 18 h for migration. For invasion, 5×10^4 cells were seeded in serum-free medium into a Matrigel invasion chamber (Becton Dickinson) for 22 h. Following incubation, the medium and cells were removed from the top chamber using cotton swabs and PBS. The number of migrating or invading cells on the underside of the membrane was determined by staining using Giemsa for 5 min. The number of migrating or invading cells in 10 fields was counted at 20× magnification using light microscopy.

Cytotoxicity assays. Capan-1 cells were resuspended in fresh medium at a concentration of 5×10^3 cells/100 μL and seeded in a 96-well plate, and cells were incubated for 48 h at 37°C. Then, GEM was added to each well at concentrations of 1, 5, 10, 50, 100, 500 and 1000 ng/mL to test the GEM treatment, or IFN-α was added to each well at concentrations of 500, 1000, 2500, 5000, 10 000, 25 000, 50 000 and 100 000 U/mL to test the IFN-α treatment. The plate was incubated at 37°C for another 48 h. For the assay, 10 μL of 3-(4,5-dimethylthiazol-2-yl)-2,5-diphenyltetrazolium bromide (MTT; 5 mg/mL) was added to each well, and the plate was incubated for an additional 3 h at 37°C. The medium and MTT solution were then aspirated, and 70 μL of DMSO (Sigma-Aldrich, St. Louis, MO, USA) was added. The absorbance was measured at 570 nm using a microplate reader.

BrdU assay. Cells (80–90% confluent) were incubated with 1 mM BrdU for 3 h at 37°C and processed using the fluorescein isothiocyanate BrdU Flow Kit (BD Biosciences) according to the manufacturer's instructions. Briefly, 1×10^6 trypsinized cells were fixed, permeabilized and digested with DNase. Cells were then stained with fluorescein isothiocyanate –conjugated anti-BrdU and 7-AAD. For cell isolation and characterization, anti-CD133/1-APC (Miltenyi Biotec) was used. For each experiment, 10^4 events were counted by flow cytometry and assays were performed in triplicate. Data were analyzed using FACSDiva.

Western blotting. Cells were lysed on ice in lysis buffer and the lysates were boiled for 5 min, clarified by centrifugation at 15 000*g* for 15 min, and then separated by SDS-PAGE. The proteins were transferred onto nitrocellulose membranes. The membranes were then incubated with a 1:200 dilution of

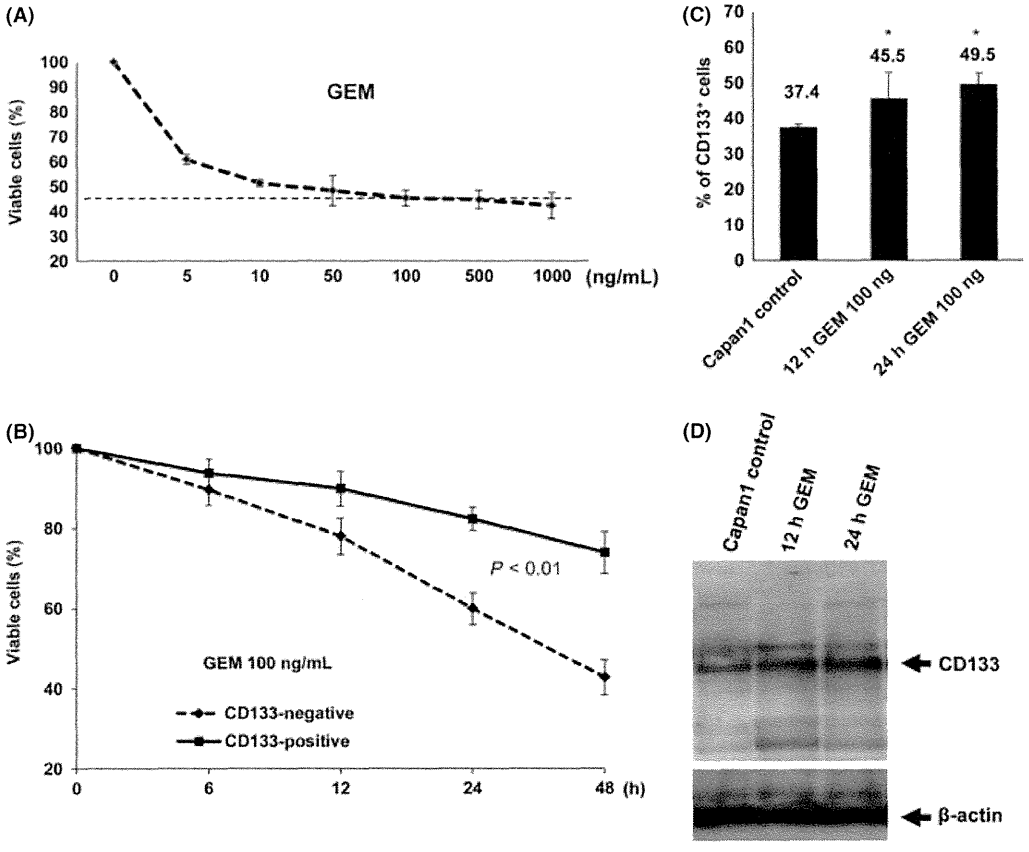

Fig. 1. CD133$^+$ Capan-1 cells are more resistant to gemcitabine (GEM) treatment than CD133$^-$ cells. (A) GEM inhibited Capan-1 cell growth in a dose-dependent manner, and its IC_{50} was 100 ng/mL. It was measured using the MTT growth inhibitory assay after 24 h of continuous GEM exposure. (B) GEM treatment (100 ng/mL) showed different sensitivities in CD133$^+$ and CD133$^-$ cells. Error bars indicate SD. (C) GEM treatment for 12 or 24 h increased the proportion of CD133$^+$ cells. Error bars indicate SD. *$P < 0.01$ *vs* control. (D) Western blot of CD133 expression.

doi: 10.1111/j.1349-7006.2012.02235.x

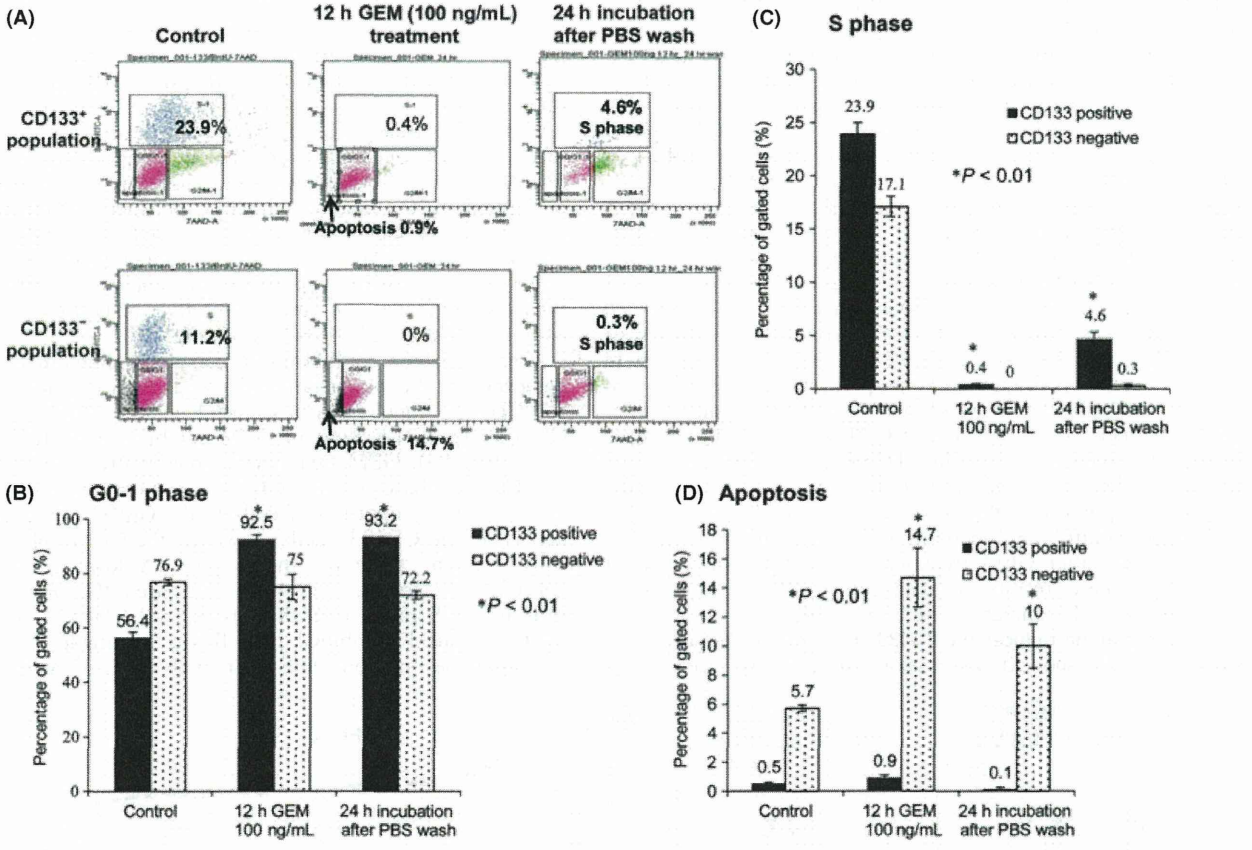

Fig. 2. Comparison of cell cycles between CD133$^+$ and CD133$^-$ cells. (A) Flow cytometry was used for cell cycle analysis before and after exposure to gemcitabine (GEM). Baseline data are provided in the left panel. Cells were then treated with GEM for 12 h (middle) followed by 24 h of recovery after withdrawal of GEM (right). (B) Comparison of CD133$^+$ and CD133$^-$ cells in the G0/G1 phase. (C) The S phase and (D) apoptosis by BrdU assay after GEM treatment. Results are based on three independent experiments. Error bars indicate SD. *$P < 0.01$ *vs* control.

anti-CD133 mAb (Miltenyi Biotec) followed by a 1:200–1000 dilution of peroxidase-conjugated anti-mouse IgG (Jackson ImmunoResearch, West Grove, PA, USA) antibody for the secondary reaction. As an internal control for the amount of protein loaded, β-actin was detected. The immunocomplex was visualized using the ECL western blot detection system (GE Healthcare Life Science, Amersham, UK).

Mitogen-activated protein kinase-integrating kinase 1 inhibition experiments. Capan-1 cells were pretreated with 20 μM CGP57380 (mitogen-activated protein kinase-integrating kinase [Mnk1] inhibitor; Sigma-Aldrich) for 60 min, and subsequently cultured with 10 μM CGP57380 during the treatment with IFN-α. Proteins were then detected with antibodies against the phosphorylated Mnk1 (Thr-197/202, 1:250 dilution; Cell Signaling Tech) and Mnk1 (1:250 dilution); 10% FCS treated cells were used as a positive control for Mnk1 phosphorylation. The signals for pMnk1 were quantified by densitometry using Image J software. To assess the effects of Mnk inhibition on cell viability, Capan-1 cells were treated with IFN-α, gemcitabine or Mnk1 inhibitor CGP57380 combination. After 48 h incubation, cell viability was determined by MTT assay.

Animal studies. The animal study was approved by the Committee on the Use of Live Animals for Teaching and Research of Kagoshima University. Non-obese diabetic (NOD)/SCID and BALB/c nu/nu (nude) mice were purchased from CLEA Japan (Tokyo, Japan).

Tumorigenic assay. For the tumorigenic assay, CD133$^+$ or CD133$^-$ populations of Capan-1 cells were collected using FACSAria and PE-conjugated anti-CD133 antibody. Freshly isolated CD133$^+$ and CD133$^-$ cells were subjected to tumorigenic assay. In total, 10, 100 and 1000 cells of each quadrant suspended in 50 μL of DMEM F-12 medium and 50 μL Matrigel were injected s.c. into 6-week-old NOD/SCID mice. Animals were maintained until death resulting from the neoplastic process or the end of the experiment. Xenograft tumors were fixed with 10% buffered formaldehyde and stained with H&E.

***In vivo* chemotherapies for xenograft tumors.** For *in vivo* treatments, nude mice were randomly assigned to four treatment groups of five mice at week 2 after s.c. injection of Capan-1 cells (5×10^5). Mice received treatments of vehicle (saline, i.p.), GEM (120 mg/kg/week, i.p.) alone, IFN-α (20 000 U/mouse/every 2 days, s.c.) alone, or GEM combined with IFN-α for 4 weeks. Growth curves of xenograft tumors in nude mice were assessed after treatments.

Statistical analysis. Group differences were analyzed statistically using the χ^2-test and Student's *t*-test. A *P*-value <0.05 was considered statistically significant. All statistical analyses were performed using StatView statistical software version 5.0 (SAS Institute, Cary, NC, USA).

Results

CD133$^+$ Capan-1 cells are resistant to gemcitabine treatment. CD133 expression was examined by flow cytometric analysis in several human pancreatic cancer cell lines. The positive ratio of CD133 in Capan-1cells is approximately 45%, higher than that in the other cell lines (Table S1), Capan-1 was chosen to evaluate the sensitivity to GEM. GEM inhibited

Capan-1 cell growth in a dose-dependent manner and its IC_{50}, as assessed by MTT growth inhibitory assay, was 100 ng/mL (Fig. 1A). The growth inhibition by GEM treatment (100 ng/mL) showed a significant ($P < 0.01$) difference between $CD133^+$ and $CD133^-$ populations of Capan-1 cells (Fig. 1B). GEM treatment increased the proportion of $CD133^+$ Capan-1 cells (Fig. 1C). Similarly, CD133 protein levels increased in a time-dependent manner (Fig. 1D). GEM treatment produced a significant increase in the G0/G1 phase and a decrease in the S phase cell populations (Fig. S1). We compared cell cycles between $CD133^+$ and $CD133^-$ populations of Capan-1 cells by BrdU assay after GEM treatment (Fig. 2A). The proportion of $CD133^+$ cells in the G0/G1 phase increased from 56.4 to 92.5%, and was maintained at 93.2% even after withdrawal of GEM (Fig. 2B). However, there were no significant changes in $CD133^+$ cells. Although the proportion of $CD133^+$ and $CD133^-$ cells in the S phase was remarkably reduced after GEM treatment, the proportion of $CD133^+$ cells in the S phase increased compared to that in $CD133^+$ cells after withdrawal of GEM (Fig. 2C). The proportion of $CD133^+$ cells in the apoptotic phase was significantly lower than that in $CD133^-$ cells under control, and apoptotic cells were highly induced in $CD133^+$ cells after GEM treatment and withdrawal of GEM (Fig. 2D). These results indicated that $CD133^+$ cells were resistant to GEM, compared to $CD133^-$ cells.

Interferon-alpha reduces the $CD133^+$ ratio of Capan-1 cells. All Capan-1 cells showed expression of IFN-α/β receptor 2 (Fig. 3A). IFN-α inhibited Capan-1 cell growth by up to 30% in a dose-dependent manner, and concentrations over 5000 U/mL showed similar inhibition rates (Fig. 3B). Importantly, IFN-α treatment decreased the proportion of $CD133^+$ cells in a time-dependent manner (Fig. S2, Fig. 3C). Similarly, after over 6 h of IFN-α treatment, CD133 protein levels were decreased (Fig. 3D). To understand the mechanism underlying IFN-α treatment, Mnk1 expression and inhibition experiment were performed. IFN-α treatment induced phosphorylation of Mnk1 in a time-dependent manner (Fig. 3E left and right). Mnk1 inhibitor CGP57380 administration antagonized the IFN-α effect on cell growth suppression, but not significantly. Mnk1 inhibitor mitigated the antiproliferative response to the co-administration of IFN-α and GEM (Fig. 3F).

Interferon-alpha contributes to combined chemotherapy with gemcitabine. We compared cell cycles between the $CD133^+$ and $CD133^-$ populations of Capan-1 cells by BrdU assay after GEM alone, IFN-α alone or GEM combined with IFN-α treatment (Fig. S3). GEM treatment increased the ratio of cells in the G0/G1 phase in the $CD133^+$ population, while IFN-α decreased the proportion of cells in the G0/G1 phase (Fig. 4A upper). In the $CD133^-$ cells, however, the G0/G1 phases were similar among these treatments (Fig. 4A lower). IFN-α, but not GEM treatment, remarkably increased the proportion of cells in the S phase in both $CD133^+$ and $CD133^-$ cells. Furthermore, GEM combined with IFN-α treatment significantly increased the apoptotic phases in both $CD133^+$ and $CD133^-$

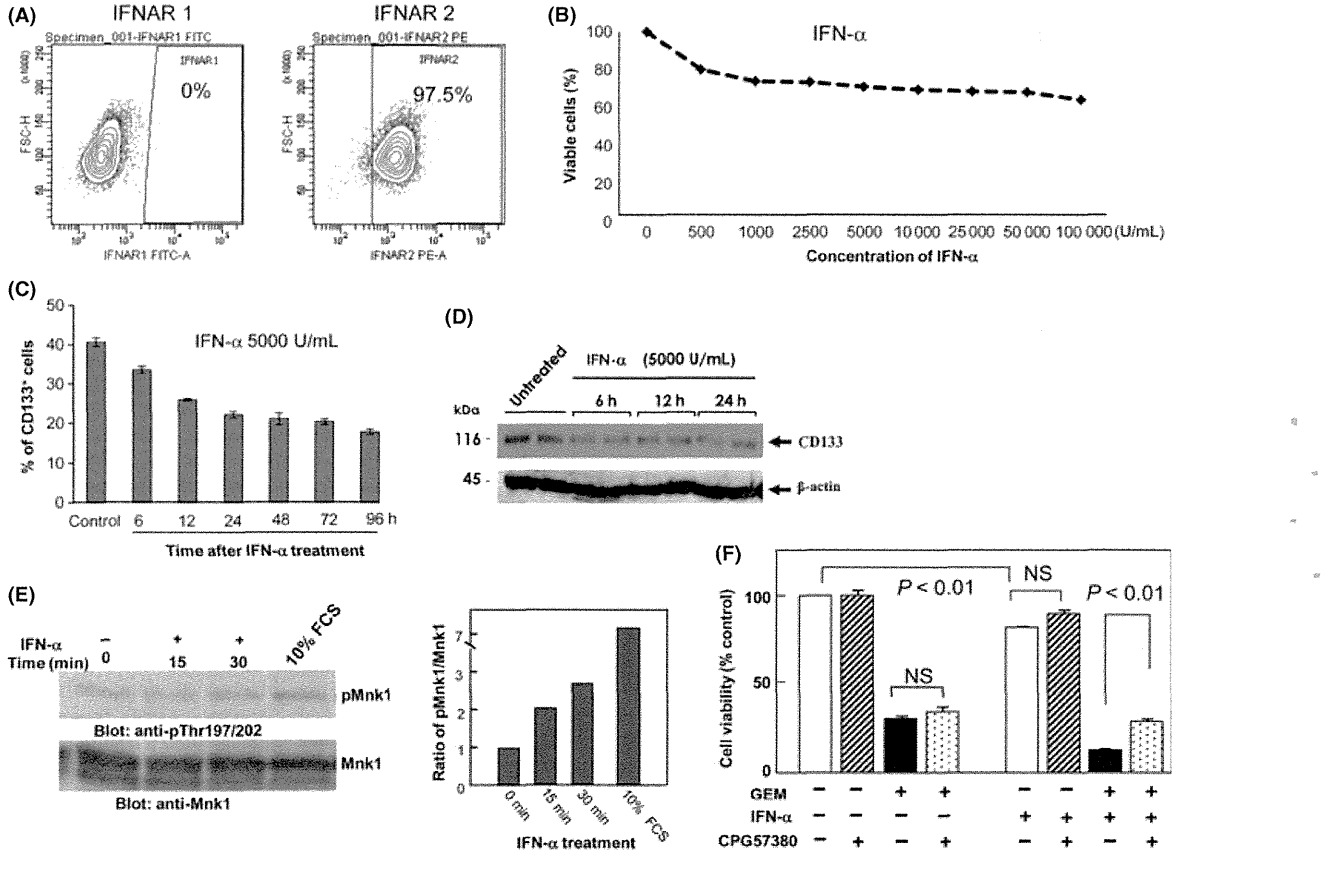

Fig. 3. Interferon-alpha (IFN-α) reduced the proportion of $CD133^+$ cells in Capan-1 cells. (A) Expressions of IFNAR 1 (left) and IFNAR 2 (right). (B) IFN-α inhibited Capan-1 cell growth in a dose-dependent manner for 48 h exposure. (C) IFN-α (5000 U/mL) treatment for 48 h decreased the proportion of $CD133^+$ cells in Capan-1 cells over time. (D) CD133 protein level analyzed by western blot. (E) IFN-α-dependent phosphorylation/activation of Mnk1 in a time-dependent manner (left and right). (F) Mnk1 mediated the antiproliferative response to the co-administration of IFN-α and gemcitabine (GEM). Capan-1 cells were treated in the combination of IFN-α, GEM and Mnk1 inhibitor CGP57380. After 48 h incubation, cell viability was determined by MTT assay. These results are the means and SD of values from four wells in one representative experiment.

doi: 10.1111/j.1349-7006.2012.02235.x

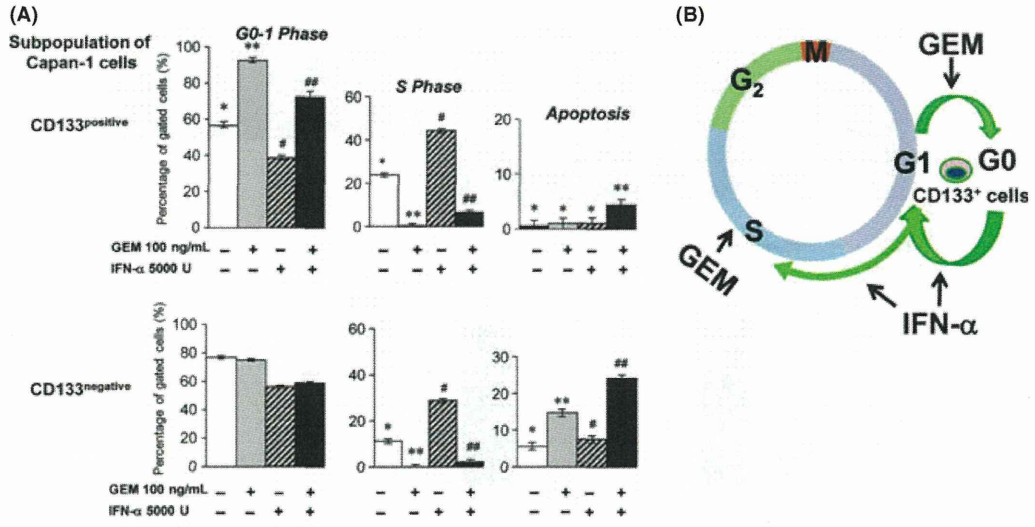

Fig. 4. Interferon-alpha (IFN-α) contributes to combined chemotherapy by reducing the proportion of the G0/G1 phase cells and increasing the proportion of the S phase and apoptotic cells. (A) Comparison of G0/G1, S and apoptotic cells by BrdU assay between $CD133^+$ and $CD133^-$ cells treated with gemcitabine (GEM) alone, IFN-α alone or GEM + IFN-α for 24 h. In $CD133^+$ (upper) and $CD133^-$ (lower) populations, * *vs* **, * *vs* # and # *vs* ## indicate $P < 0.01$. Error bars indicate SD. (B) Model of IFN-α modulating $CD133^+$ cells from G0/G1 to the S phase and targeting them combined with GEM.

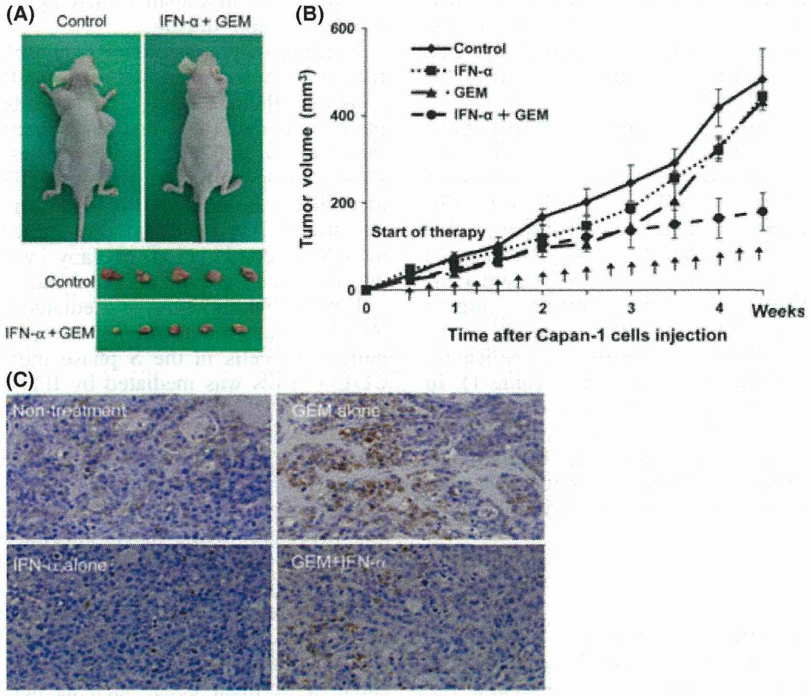

Fig. 5. Effect of interferon-alpha (IFN-α) on the growth of xenograft Capan-1 tumor in nude mice. (A) Xenograft tumors with IFN-α + gemcitabine (GEM) treatment were smaller than those with controls in nude mice. (B) Tumor growth curves of Capan-1 xenografts which were treated with GEM (100 ng/mL) alone, IFN-α (5000 U/mL) alone or GEM plus IFN-α. IFN-α + GEM treatment showed a significant effect ($P < 0.01$). (C) Comparison of histological CD133 expression in Capan-1 xenografts with treatments at week 5 after inoculation into nude mice.

cells (Fig. 4A). These results suggest that IFN-α modulates the cell cycle of $CD133^+$ Capan-1 cells (Fig. 4B).

Effect of interferon-alpha on xenograft tumors of $CD133^+$ cells. We attempted to determine the *in vivo* effect of IFN-α on xenograft tumors derived from Capan-1 cells in nude mice. Four weeks' treatment of GEM combined with IFN-α suppressed tumor growth in nude mice (Fig. 5A) and led to significant differences in tumor growth curves compared to the control, GEM alone or IFN-α alone (Fig. 5B). However, body weight did not change significantly (Fig. S4A). In the immunohistological study, xenograft tumor cells treated with GEM showed higher $CD133^+$ expression than those of the control. In

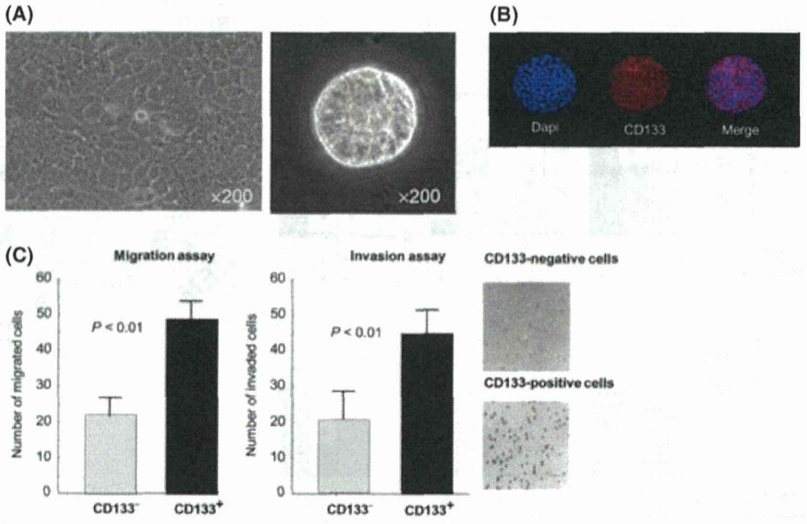

Fig. 6. Cancer stem-like characteristics were identified in CD133$^+$ Capan-1 cells. (A) Capan-1 cells showed monolayer growth in medium with serum (left). In serum-free culture, a sphere was generated after 10 days of culture (right). Magnification: ×200. (B) These sphere cells expressed CD133 by immunofluorescence staining. Magnification: ×200. (C) Comparison of migration and invasion abilities between CD133$^+$ and CD133$^-$ Capan-1 cells.

contrast, CD133$^+$ expression in xenograft tumors treated with IFN-α alone was lower than those with saline as control. Interestingly, xenograft tumors treated with GEM combined with IFN-α showed an intermediate CD133$^+$ expression (Fig. 5C). The flow cytometric analysis showed similar results to the immunohistological study (Fig. S4B).

CD133$^+$ Capan-1 cells identified as a cancer stem-like population of cells. Flow cytometric analysis was performed on several human pancreatic cancer cell lines. Among these, Capan-1 showed high expression of CD133 (Table S1, Fig. 6A). Capan-1 cells showed sphere formations in a stem cell-permissive medium without serum (Fig. S5A), and CD133 was expressed on the cell surface or in the cytoplasm in these sphere cells (Fig. 6B). These CD133$^+$ Capan-1 cells showed a higher potential of migration and invasion than CD133$^-$ cells (Fig. 6C). Furthermore, CD133$^+$ cells showed significantly greater tumorigenic potential than CD133$^-$ cells (Table 1). In these tumors, the histology was ductal adenocarcinoma and CK expression was observed in all tumor cells, while CD133 expression was shown in a part of the tumor cells by immunohistological staining (Fig. S5B). These results indicate that the CD133$^+$ population of Capan-1 cells exhibits CSC-like properties.

Discussion

Gemcitabine had greater inhibitory effects on the human pancreatic cancer cells, Capan-1. However, CD133$^+$ cells showed more resistance to GEM than CD133$^-$ cells, although the growth speed between CD133$^+$ and CD133$^-$ cells was the same in Capan-1. Along with GEM treatment, the ratio of CD133$^+$ cells in Capan-1 increased and the resistance against GEM was more drastic.

Interferon-alpha modulated the cell cycle, resulting in antiproliferative and proapoptotic effects on CD133$^+$ cells using combined therapy with GEM. Members of the IFN family are pleiotropic cytokines that have been shown to be important regulators of cell growth. IFN-α has been recognized to have therapeutic potential for the prevention and treatment of hepatocellular carcinoma.[27,28] Whether pancreatic cancer cells respond to IFN treatment is unknown, although clinical trials including combination therapy with IFN-α for advanced pancreatic cancer patients have had promising results.[29,30]

Type I IFN signaling is mediated by activation of the JAK-STAT signaling pathway.[31] In our study, the increase of the number of cells in the S phase indicates that proliferation of CD133$^+$ cells was mediated by IFN-α treatment. The accumulation of CD133$^+$ cells into the G0/G1 phase was remarkably increased after GEM treatment. GEM is a nucleoside analog that can replace one of the building blocks of the nucleic acid during DNA replication, leading to suppression tumor growth. Another target of GEM is to inactivate the enzyme ribonucleotide reductase. GEM shows specificity for proliferation in the S phase of the cell cycle with no effect on progress through early G1, G2 or M phases of the cell cycle.[32] However, IFN-α contributed to the effect on the decrease of CD133$^+$ cells in the G0/G1 phase and the increase of them in the S phase. IFN-α priming provides an efficient way to induce cell cycle entry of dormant cells, such as hematopoietic stem cells.[33] IFN-α makes dormant cells susceptible to elimination by antiproliferative chemotherapeutic drugs,[34] such as CD133$^+$ cells, as shown in Figure 4B. According to a recent report, the Mnk/eIF4E kinase pathway is activated in an IFN-inducible manner and plays important roles in mRNA translation for IFN-stimulated genes and in the generation of IFN-inducible antiproliferative responses.[35] In our study, IFN-α treatment induced rapid phosphorylation of Mnk1 that was detectable within 15 min of treatment. Mnk1 inhibitor may mitigate the antiproliferative response to the co-administration of IFN-α and GEM. Further clarification of tumor suppression by IFN-α is necessary.

Table 1. Comparison of tumorigenesis between CD133$^+$ and CD133$^-$ population cells in Capan-1 using non-obese diabetic/SCID mice

Subset of Capan-1	Number of implanted cells			Total
	10	10^2	10^3	
CD133$^+$	1/10 (10%)	7/10** (70%)	8/10** (80%)	16/30*** (53%)
CD133$^-$	0/10	0/10	1/10 (10%)	1/30 (3%)

***$P < 0.001$; **$P < 0.05$.

doi: 10.1111/j.1349-7006.2012.02235.x

Numerous studies have identified a "side population" (SP) in various tumor types,[36–39] and SP cells seem to be rich in stem cells.[24] These malignant SP cells proliferate in a sustained fashion and readily export many cytotoxic drugs. This high drug efflux capacity correlates with the strong expression of ATP-binding cassette transporters.[36] Interestingly, ovarian cancer containing SP cells have been found to be IFN-α sensitive *in vitro* and *in vivo* due to marked anti-proliferative and pro-apoptotic effects.[20] In this study, however, the $CD133^+$ population of Capan-1 cells did not coincide with the SP population (data not shown). IFN-α increased the number of $CD133^+$ cells in the S phase compared to that of $CD133^-$ cells. Furthermore, IFN-α combined with GEM induced apoptosis in both $CD133^+$ and $CD133^-$ cells to a greater extent than GEM or IFN-α treatment alone. IFN-α has also been shown to induce differentiation of lung cancer cells [37] and hepatic progenitors.[40] In addition, IFN-α has been shown to regulate the transition from SP into other phenotypes, although this IFN signaling-related mechanism is unclear.[25]

In our study, the combination of IFN-α and GEM significantly inhibited the growth of xenografts of Capan-1 cells compared to the control, GEM or IFN-α alone. These results were consistent with the *in vitro* data. However, using *in vivo* orthotopic pancreas cancer models, the combination of IFN-α and GEM has been reported to synergistically induce endothelial cell apoptosis.[26] These results suggest that IFN-α may have multiple biological functions in the modulation of gene expression and regulation of the cell cycle in terms of tumor suppression *in vivo*.

In contrast, $CD133^+$ population of Capan-1 cells exhibited greater tumorigenesis and the potential to generate spheres and aggressive behavior, such as migration and invasion, compared with $CD133^-$ cells. These results suggest that CD133 plays an important role in the cancer stem-like population of Capan-1 cells. Hence, the underlying mechanism of the CSC regulation is an important issue. In a recent study, the combined blockade of sonic hedgehog and mTOR signaling together with GEM treatment led to a profound depletion of the CSC compartment and shrinkage of established tumors.[41] Our results shed new light on the impact of IFN-α on the cell cycle of a CSC-like population in pancreatic cancer cells, although further research into the mechanism of the CSC modulation by IFN-α is still needed.

In the present study, we demonstrated that GEM could efficiently act on S phase cells in both $CD133^+$ and $CD133^-$. $CD133^+$ cells could escape from GEM treatment by retention in the G0/G1 phase. IFN-α administration prompted G0/G1 phase $CD133^+$ cells to re-enter the cell cycle. Thus, IFN-α treatment could increase GEM therapeutic efficacy. Moreover, GEM combined therapy with IFN-α significantly suppressed xenograft tumor growth. In addition, $CD133^+$ cells showed CSC-like properties, such as generation of spheres in serum-free culture and tumorigenesis in NOD/SCID mice. Taken together, IFN-α, as a modulator, could contribute to the treatment of $CD133^+$ cancer cells with CSC-like properties and be effective in combined chemotherapies for pancreatic cancer stem-like cells.

Acknowledgment

This work was supported by grants-in-aid for scientific research from the Ministry of Education, Science, Sports, and Culture, Japan.

Disclosure Statement

The authors have no conflict of interest to declare.

References

1 Jemal A, Siegel R, Ward E, Hao Y, Xu J, Thun MJ. Cancer statistics, 2009. *CA Cancer J Clin* 2009; **59**: 225–49.
2 Reya T, Morrison SJ, Clarke MF, Weissman IL. Stem cells, cancer, and cancer stem cells. *Nature* 2001; **414**: 105–11.
3 Hanahan D, Weinberg RA. Hallmarks of cancer: the next generation. *Cell* 2011; **144**: 646–74.
4 Dean M. Cancer stem cells: implications for cancer causation and therapy resistance. *Discov Med* 2005; **5**: 278–82.
5 Eyler CE, Rich JN. Survival of the fittest: cancer stem cells in therapeutic resistance and angiogenesis. *J Clin Oncol* 2008; **26**: 2839–45.
6 Singh SK, Hawkins C, Clarke ID *et al.* Identification of human brain tumour initiating cells. *Nature* 2004; **432**: 396–401.
7 Beier D, Hau P, Proescholdt M *et al.* CD133(+) and CD133(−) glioblastoma-derived cancer stem cells show differential growth characteristics and molecular profiles. *Cancer Res* 2007; **67**: 4010–5.
8 Zhao P, Lu Y, Jiang X, Li X. Clinicopathological significance and prognostic value of CD133 expression in triple-negative breast carcinoma. *Cancer Sci* 2011; **102**: 1107–11.
9 Collins AT, Berry PA, Hyde C, Stower MJ, Maitland NJ. Prospective identification of tumorigenic prostate cancer stem cells. *Cancer Res* 2005; **65**: 10946–51.
10 Florek M, Haase M, Marzesco AM *et al.* Prominin-1/CD133, a neural and hematopoietic stem cell marker, is expressed in adult human differentiated cells and certain types of kidney cancer. *Cell Tissue Res* 2005; **319**: 15–26.
11 Ferrandina G, Bonanno G, Pierelli L *et al.* Expression of CD133-1 and CD133-2 in ovarian cancer. *Int J Gynecol Cancer* 2008; **18**: 506–14.
12 Zhu Z, Hao X, Yan M *et al.* Cancer stem/progenitor cells are highly enriched in CD133 + CD44 + population in hepatocellular carcinoma. *Int J Cancer* 2010; **126**: 2067–78.
13 O'Brien CA, Pollett A, Gallinger S, Dick JE. A human colon cancer cell capable of initiating tumour growth in immunodeficient mice. *Nature* 2007; **445**: 106–10.
14 Ricci-Vitiani L, Lombardi DG, Pilozzi E *et al.* Identification and expansion of human colon-cancer-initiating cells. *Nature* 2007; **445**: 111–5.
15 Haraguchi N, Ohkuma M, Sakashita H *et al.* CD133+ CD44+ population efficiently enriches colon cancer initiating cells. *Ann Surg Oncol* 2008; **15**: 2927–33.
16 Morikawa K, Okudo K, Haraguchi N *et al.* Combination use of anti-CD133 antibody and SSA lectin can effectively enrich cells with high tumorigenicity. *Cancer Sci* 2011; **102**: 1164–70.
17 Maeda S, Shinchi H, Kurahara H *et al.* CD133 expression is correlated with lymph node metastasis and vascular endothelial growth factor-C expression in pancreatic cancer. *Br J Cancer* 2008; **98**: 1389–97.
18 Hermann PC, Huber SL, Herrler T *et al.* Distinct populations of cancer stem cells determine tumor growth and metastatic activity in human pancreatic cancer. *Cell Stem Cell* 2007; **1**: 313–23.
19 Burris HA III, Moore MJ, Andersen J *et al.* Improvements in survival and clinical benefit with gemcitabine as first-line therapy for patients with advanced pancreas cancer: a randomized trial. *J Clin Oncol* 1997; **15**: 2403–13.
20 Stark GR, Kerr IM, Williams BRG, Silverman RH, Schreiber RD. How cells respond to interferons. *Ann Rev Biochem* 1998; **67**: 227–64.
21 Tagliaferri P, Caraglia M, Budillon A *et al.* New pharmacokinetic and pharmacodynamic tools for interferon-α (IFN-α) treatment of human cancer. *Cancer Immunol Immunother* 2005; **54**: 1–10.
22 Gresser I, Belardelli F. Endogenous type I interferons as a defense against tumors. *Cytokine Growth Factor Rev* 2002; **13**: 111–8.
23 Dunn GP, Koebel CM, Schreiber RD. Interferons, immunity and cancer immunoediting. *Nat Rev Immunol* 2006; **6**: 836–48.
24 Challen GA, Little MH. A side order of stem cells: the SP phenotype. *Stem Cells* 2006; **24**: 3–12.
25 Moserle L, Indraccolo S, Ghisi M *et al.* The side population of ovarian cancer cells is a primary target of IFN-α antitumor effects. *Cancer Res* 2008; **68**: 5658–68.
26 Solorzano CC, Hwang R, Baker CH *et al.* Administration of optimal biological dose and schedule of interferon alpha combined with gemcitabine induces apoptosis in tumor-associated endothelial cells and reduces growth of human pancreatic carcinoma implanted orthotopically in nude mice. *Clin Cancer Res* 2003; **9**: 1858–67.
27 Miyamoto A, Umeshita K, Sakon M *et al.* Advanced hepatocellular carcinoma with distant metastases, successfully treated by a combination therapy

of alpha-interferon and oral tegafur/uracil. *J Gastroenterol Hepatol* 2000; **15**: 1447–51.
28 Wada H, Nagano H, Yamamoto H *et al.* Combination therapy of interferon- and 5-fluorouracil inhibits tumor angiogenesis in human hepatocellular carcinoma cells by regulating vascular endothelial growth factor and angiopoietins. *Oncol Rep* 2007; **18**: 801–9.
29 Sparano JA, Lipsitz S, Wadler S *et al.* Phase II trial of prolonged continuous infusion of 5-fluorouracil and interferon-α in patients with advanced pancreatic cancer. Eastern Cooperative Oncology Group Protocol 3292. *Am J Clin Oncol* 1996; **19**: 546–51.
30 Wagener DJ, Wils JA, Kok TC, Planting A, Couvreur ML, Baron B. Results of a randomized phase II study of cisplatin plus 5-fluorouracjl versus cisplatin plus 5-fluorouracil with a-interferon in metastatic pancreatic cancer. An EORTC gastrointestinal tract cancer group trial. *Eur J Cancer* 2002; **38**: 648–53.
31 Martínez CC, Alvarez SN, Vicente OV, García RJ, Pascual CF, Campos AM. In vitro and in vivo effect of IFN-αlpha on B16F10 melanoma in two models: subcutaneous (C57BL6J mice) and lung metastasis (Swiss mice). *Biomed Pharmacother* 2009; **63**: 305–12.
32 Hertel LW, Boder GB, Kroin JS *et al.* Evaluation of the antitumor activity of gemcitabine (2′,2′-difluoro-2′-deoxycytidine). *Cancer Res* 1990; **50**: 4417–22.
33 Essers MA, Offner S, Blanco Bose WE *et al.* IFNα activates dormant haematopoietic stem cells in vivo. *Nature* 2009; **458**: 904–8.
34 Persano L, Moserle L, Esposito G *et al.* Interferon-alpha counteracts the angiogenic switch and reduces tumor cell proliferation in a spontaneous model of prostatic cancer. *Carcinogenesis* 2009; **30**: 851–60.
35 Joshi S, Kaur S, Redig AJ *et al.* Type 1 interferon (IFN)-dependent activation of Mnk1 and its role in the generation of growth inhibitory responses. *Proc Natl Acad Sci USA* 2009; **106**: 12097–102.
36 Hirschmann-Jax C, Foster AE, Wulf GG *et al.* A distinct "side population" of cells with high drug efflux capacity in human tumor cells. *Proc Natl Acad Sci USA* 2004; **101**: 14228–33.
37 Kondo T, Setoguchi T, Taga T. Persistence of a small subpopulation of cancer stem-like cells in the C6 glioma cell line. *Proc Natl Acad Sci USA* 2004; **101**: 781–6.
38 Chiba T, Kita K, Zheng YW *et al.* Side population purified from hepatocellular carcinoma cells harbors cancer stem cell-like properties. *Hepatology* 2006; **44**: 240–51.
39 Haraguchi N, Utsunomiya T, Inoue H *et al.* Characterization of a side population of cancer cells from human gastrointestinal system. *Stem Cells* 2006; **24**: 506–13.
40 Lim R, Knight B, Patel K, McHutchison JG, Yeoh GC, Olynyk JK. Antiproliferative effects of interferon alpha on hepatic progenitor cells in vitro and in vivo. *Hepatology* 2006; **43**: 1074–83.
41 Mueller MT, Hermann PC, Witthauer J *et al.* Combined targeted treatment to eliminate tumorigenic cancer stem cells in human pancreatic cancer. *Gastroenterology* 2009; **137**: 1102–13.

Supporting Information

Additional Supporting Information may be found in the online version of this article:

Fig. S1. Flow cytometric analysis of cell cycle progression in Capan-1 cells treated with gemcitabine (100 ng/mL) for 12 or 24 h.

Fig. S2. Flow cytometric analysis of CD133 expression in Capan-1 cells treated with or without interferon-alpha (IFN-α). IFN-α treatment (5000 IU/mL) for 24 h decreased the ratio of $CD133^+$ Capan-1 cells over time.

Fig. S3. Comparison of BrdU assay between $CD133^+$ and $CD133^-$ Capan-1 cells treated with gemcitabine (GEM) (100 ng/mL) alone, interferon-alpha (IFN-α) (5000 U/mL) alone or GEM combined with IFN-α for 24 h.

Fig. S4. (A) Body weight curves of nude mice were not significantly different among the three treatments, which were gemcitabine (GEM) (100 ng/mL) alone, interferon-alpha (IFN-α) (5000 U/mL) alone or GEM plus IFN-α. (B) Comparison of proportions of $CD133^+$ cells in Capan-1 xenografts that were treated with GEM (100 ng/mL) alone, IFN-α (5000 U/mL) alone or GEM plus IFN-α at week 2 and 5.

Fig. S5. (A) Comparison of the number of spheres per well (cm^3) for pancreatic cancer cell lines, Panc-1, Capan-1, MIA PaCa-2, PK45H and SW1990. The white and black bars indicate the spheres composed of 3–30 and >30 cells, respectively. (B) Immunohistochemical study of a Capan-1 tumor generated by transplantation into non-obese diabetic (NOD)/SCID mice. (i) HE staining and (ii, iii, iv) immunostaining performed to identify cytokeratin (CK) and CD133 expression, respectively.

Table S1. Comparison of potential markers related to tumor-initiating cells in six pancreatic cancer cell lines.

Please note: Wiley-Blackwell are not responsible for the content or functionality of any supporting materials supplied by the authors. Any queries (other than missing material) should be directed to the corresponding author for the article.

doi: 10.1111/j.1349-7006.2012.02235.x

Human Cell (2012) 25:1–8
DOI 10.1007/s13577-011-0037-9

RESEARCH ARTICLE

Establishment of a highly migratory subclone reveals that CD133 contributes to migration and invasion through epithelial–mesenchymal transition in pancreatic cancer

Qiang Ding · Makoto Yoshimitsu · Taisaku Kuwahata · Koki Maeda · Tomomi Hayashi · Toru Obara · Yumi Miyazaki · Shyuichiro Matsubara · Shoji Natsugoe · Sonshin Takao

Received: 25 July 2011 / Accepted: 20 October 2011 / Published online: 23 November 2011

Abstract Pancreatic cancer is a lethal disease because of invasion and early metastasis. Although CD133, a marker of cancer stem cells (CSCs) in a variety of solid tumors, has been studied in recent decades, its function remains obscure. Recent reports suggest that epithelial–mesenchymal transition (EMT) may be related to the properties of CSCs. In this study, we investigated whether CSC markers are associated with EMT. For Capan1M9, a highly migratory cell subclone established from human pancreatic cancer cell line Capan-1, CD133 expression, migration, and invasion were greater than for the parent cells. In Capan1M9 cells, the EMT-related transcription factors Slug and Snail were up-regulated, and N-cadherin and fibronectin were also substantially increased. In contrast, occludin and desmoplakin were suppressed. Knockdown of endogenous CD133 in the Capan1M9 cells led to Slug suppression and reduction of migration and invasion. Taken together, CD133 has an important role in migration and invasion by facilitating EMT in pancreatic cancer cells.

Keywords Epithelial–mesenchymal transition (EMT) · CD133 · Migration · Slug · Pancreatic cancer

Introduction

Pancreatic cancer is an exceptionally devastating and incurable disease because of early local invasion and distant metastasis to the lymph nodes and liver [1]. Most pancreatic cancers at diagnosis are advanced and unresectable, and very little effective therapy can currently be offered to patients. Therefore, it is critical to understand the molecular mechanism of invasion and metastasis [2].

Metastasis involves several processes, including cancer cell detachment from the primary tumor, local invasion, dissemination through surrounding blood vessels or lymphatic vessels, and attachment and proliferation at the metastatic site [3]. Although metastasis is a complicated process involving multiple factors and genetic events, increased migratory and invasive capabilities are critical to initiation of the process [4, 5]. During cancer progression, some cells within the primary tumor may reactivate a latent embryonic program known as epithelial–mesenchymal transition (EMT), thereby acquiring increased motility and invasiveness; this facilitates invasion of both local and distant tissues by cancerous cells [6]. During EMT, cells lose their epithelial characteristics, including cell adhesion and polarity [7, 8], and acquire a mesenchymal morphology and the ability to migrate. EMT is a recognized mechanism for dispersing cells during embryonic development [9], tissue regeneration [10], and initiation of invasive and metastatic

Electronic supplementary material The online version of this article (doi:10.1007/s13577-011-0037-9) contains supplementary material, which is available to authorized users.

Q. Ding · T. Kuwahata · K. Maeda · T. Obara · Y. Miyazaki · S. Matsubara · S. Takao (✉)
Division of Cancer and Regenerative Medicine, Frontier Science Research Center, Kagoshima University Graduate School of Medical and Dental Sciences, 8-35-1 Sakuragaoka, Kagoshima 890-8520, Japan
e-mail: sonshin@m2.kufm.kagoshima-u.ac.jp

M. Yoshimitsu
Department of Hematology and Immunology, Kagoshima University Graduate School of Medical and Dental Sciences, 8-35-1 Sakuragaoka, Kagoshima 890-8520, Japan

K. Maeda · T. Hayashi · S. Natsugoe
Department of Digestive Surgery, Kagoshima University Graduate School of Medical and Dental Sciences, 8-35-1 Sakuragaoka, Kagoshima 890-8520, Japan

behavior in epithelial cancer [11–13]. Local invasion is believed to be an initial and essential step leading to the generation of usually fatal distant metastases [3, 11].

CD133 (prominin-1) is a cell membrane protein first found in hematopoietic stem cells and early progenitor cells in the bone marrow [14]. It has recently been used extensively as a marker to identify stem cells from normal and cancerous tissue [15–17]. However, evidence also suggests that CD133 expression is not restricted to cancer stem cells (CSCs). For example, in rat glioma cell line C6, both $CD133^+$ and $CD133^-$ subpopulations had clonogenic, self-renewal, and tumorigenic capacity [18]. Several signaling pathways have been shown to regulate CD133 epitope-positive cells. For example, the Notch, Hedgehog, and bone morphogenic protein (BMP) signaling pathways have been shown to be dependent on the tissue-specific expression of splice variants of prominin-family molecules [17, 19]. Taken together, these data suggest that further investigation is still needed to understand the biological role of CD133 in cancer development.

We have previously reported a significant correlation between CD133 expression and clinicopathologic factors, histological type, lymphatic invasion, and lymph node metastasis in patients with pancreatic cancer who underwent a curative operation [2]. Therefore, it is plausible that CD133 is involved in migration and invasion. Because EMT consists of sequential multistep programs during tumor metastasis, an appropriate method or in-vitro cell line is needed for further elucidation of this complicated program. In this study, a highly migratory and invasive cell line was established from the pancreatic cancer cell line, Capan-1, to investigate the mechanism involved in migration and to identify further promising targets for preventing metastasis.

Materials and methods

Cell culture

Human pancreatic cancer cell line, Capan-1, was purchased from the American Type Culture Collection (ATCC, VA, USA) and cultured in DMEM/F12 (Sigma, MO, USA) medium containing 10% fetal bovine serum (FBS; Invitrogen, CA, USA) supplemented with 100 units/ml penicillin and 100 mg/ml streptomycin, followed by incubation at 37°C under a humidified atmosphere containing 5% CO_2. Cell growth rate was examined by cell counting.

Selection of migratory subclones from the Capan-1 cell line

Figure 1 outlines the procedure used for selecting the migratory subclones. Cells (2×10^5) suspended in serum-free medium were seeded into a single well of a 24-well cell-culture insert (8.0 μm pore size), and the insert was placed into plates containing 10% FBS as chemoattractant. The plate was incubated for 18 h at 37°C in 5% CO_2. Migrating cells were collected from the underside of the membrane by use of Accutase™ (Millipore, MA, USA), seeded into the 24-well plate again, and expanded into a 35 cm^2 flask; these cells were designated Capan1M1. When the selected cells were confluent, an aliquot (5×10^4 cells/well) was applied to another migration insert and migrating cells were collected as described above. In total, the procedure was repeated 9 times, and two to threefold repeatable differences in migration and invasion were achieved.

Migration and invasion assays

Cells ($2–5 \times 10^4$) were seeded, in serum-free medium, into 24-well BD Falcon migration inserts (8 μm pore size) for migration or into a BD BioCoat Matrigel invasion chamber (BD Biosciences, NJ, USA). Inserts were placed into plates containing 10% FBS as chemoattractant and incubated for 18 h for migration and 24 h for invasion. After incubation, media plus cells were removed from the top chamber by use of cotton swabs and phosphate-buffered saline (PBS). The membrane with cells was stained with Giemsa for 5 min. The number of migrating or invading cells in 10 fields was counted at 20× magnification by light microscopy. Data were calculated as mean ± SD.

Wound-healing assay

CytoSelect™ 24-well wound-healing assay (Cell Biolabs, CA, USA) was used as the migration assay. Wound field was generated according to the product manual. Cell sus-

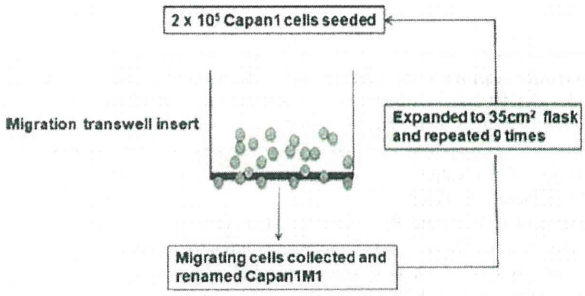

Fig. 1 Selection of Capan1M9 migratory subclone by use of the migration transwell insert. For the first round of selection a total of 2×10^5 Capan-1 parental cells were seeded into a 24-well migration transwell insert and incubated for 18 h. Migrating cells were collected from the bottom of the membrane by use of Accutase™, plated into the 24-well plate, expanded into a 35 cm^2 flask, and renamed Capan1M1. When confluent, the cells were subjected to further rounds of selection by repeating the migration assay. In total, the procedure was repeated 9 times and the cells were designated Capan1M9

pension was added to the well with the insert in place then incubated for 24–48 h. The cells were then cultured until a monolayer formed and the insert was removed to generate a "wound field". Cells were monitored, under a microscope, for migration into the wound field until the wound closed. Wound-healing area was calculated by use of Axiovision Rel software (Zeiss, Germany).

Immunofluorescence staining

Immunofluorescence staining was performed on primary adherent cultures of Capan-1 cells. After fixing with 10% formalin the cells were incubated with primary antibody staining for 2 h in an incubator at 37°C with anti-E-cadherin and vimentin (Santa Cruz, CA, USA) then washed three times with PBS and 2% FBS. This was followed by incubation for 1 h with Alexa Fluor® goat anti-mouse secondary antibody (Invitrogen). DAPI nuclear staining was performed for a further 5 min and an additional three washes. These stained cells were viewed by fluorescent microscopy (Zeiss). Primary antibodies were replaced by PBS in the negative control group.

Cell lysis and immunoblotting

Cells were lysed on ice in lysis buffer and the lysates were boiled for 5 min, clarified by centrifugation at 15000*g* for 15 min, and separated by SDS-PAGE. The proteins were transferred on to nitrocellulose membranes. The membranes were incubated with a 1:100–200 dilution of the following human polyclonal or monoclonal antibodies: E-cadherin, vimentin, N-cadherin, Slug (Santa Cruz), fibronectin (R&D, MN, USA), desmoplakin, occludin, Snail (Abcam, MA, USA), and CD133 (Miltenyi Biotec, Germany) followed by 1:200–1000 dilution of peroxidase-conjugated anti-goat IgG, anti-rabbit IgG (Santa Cruz) or anti-mouse IgG (Jackson Immunoresearch, PA, USA) antibody for the secondary reaction. As an internal control for the amount of protein loaded, β-actin was detected by use of a specific antibody (Sigma). The immunocomplex was visualized by use of the ECL Western blot detection system (Amersham, UK).

Real-time quantitative RT-PCR (ABI)

Total RNA (tRNA) was extracted by use of an RNeasy extraction kit (Qiagen, Germany). Primers and probes were obtained from Applied Biosystems™ (Life Technologies, CA, USA) as Assay-on-Demand Gene Expression Products. Real-time RT-PCRs were conducted in accordance with the supplier's directions. PCR mixture (20 µl) contained 10 µl 2× Taqman Universal PCR Master Mix, 1 µl 20× working stock of gene expression assay mix, and 20 µg tRNA. Real-time RT-PCRs were done in a StepOne Real-time PCR system (Applied Biosystems, CA, USA). The reaction for each sample was conducted in triplicate. Fluorescence of the PCR products was detected by use of the same apparatus. The number of cycles for the amplification plot to reach the threshold limit (C_t value) was used for quantification. Glyceraldehyde-3-phosphate dehydrogenase (GAPDH) was used for normalization.

Capan1M9-GFP-shCD133 cell line established by lentiviral transduction

pLVTHM is a second-generation lentiviral vector which engineers shRNA under H1 promoter (Addgene, MA, USA) and co-expresses enGFP under the elongation factor 1α promoter. CD133 shRNA 877 sense (5′-cgcgtccccggacaaggcgttcacagatttcaagagaatctgtgaacgccttgtccttttggaaat-3′) and CD133 shRNA 877 antisense (5′-cgatttccaaaaaggacaaggcgttcacagattctcttgaaatctgtgaacgccttgtccgggga-3) oligonucleotides were annealed to each other and ligated into the pLVTHM vector at the *Cla*I and *Mlu*I sites, which yields pLVTHM-CD133-877 shRNA transfer vector. 293T cells were co-transfected with 4 µg pLVTHM-CD133-877 shRNA transfer plasmid, 3 µg psPAX2 packaging plasmid, and 1 µg pMD2.G envelope plasmid by use of Fugene 6 transfection reagent (Roche, CA, USA). Twenty-four hours after transfection the medium was replaced with fresh DMEM + 10% FBS. Forty-eight hours after transfection, viral supernatant was harvested and filtered through a 0.45-µm filter. Capan1M9 cells expressing CD133 were transduced with filtered viral supernatant containing 8 µg/ml protamine sulfate 72 h after transfection. Flow-cytometric analysis was performed with a FACSCan (BD Biosciences, CA, USA) for enGFP expression. enGFP-positive cell fractions were then sorted by use of a FACSAria (BD Biosciences). The purity of the fractions routinely exceeded 95%. CD133-PE, CD44-APC, and CD24-FITC antibody (Miltenyi, Germany) were used for flow-cytometric analysis.

Statistical analysis

Group differences were analyzed statistically by use of Student's t test ($p < 0.05$ was considered statistically significant) in StatView statistical software version 5.0 (SAS Institute, NC, USA).

Results

Selection of a migratory subclone, Capan1M9, from the Capan-1 parental cell line

For cultured Capan-1 cells, tightly packed clusters in a monolayer growth pattern and a variety of cell shapes were